Environmental Processes (2020) 7:479–492
https://doi.org/10.1007/s40710-020-00429-4

ORIGINAL ARTICLE

Adsorptive Removal of Remazol Brilliant Blue R from Water by Using a Macroporous Polystyrene Resin: Isotherm and Kinetic Studies

Gulseren Ozturk[1] · Hulya Silah[1]

Received: 7 October 2019 / Accepted: 2 April 2020 / Published online: 19 April 2020

Abstract

The pollution of surface and drinking water with dyes is one growing problem. The present manuscript explains the application of a macroporous polystyrene resin called Amberlyst A21, as a new effective adsorbent in the removal of Remazol Brilliant Blue R dye from aqueous solutions. The Remazol Brilliant Blue R adsorption on the Amberlyst A21 was characterized based on various parameters such as solution pH, initial dye concentration, contact time and adsorbent dosage. The best adsorption conditions were: solution pH 2, contact time 150 min, Amberlyst A21 dosage of 1.0 g/L at 25 °C. The morphology of Amberlyst A21 was analyzed by FTIR and SEM techniques. Amberlyst A21 exhibited enhanced Remazol Brilliant Blue R removal behavior with maximum adsorption capacity of 208.33 mg/g based on the Langmuir isotherm model, which was higher than those of other previously reported adsorbents. Kinetic investigations showed that a pseudo-first order model was more suitable than the pseudo-second order model. The results indicate that Amberlyst A21, as an adsorbent, has great potential especially in the area of dye removal.

Keywords Amberlyst A21 · Remazol Brilliant Blue R · Resin · Adsorption · Isotherms · Kinetics

Article Highlights
- Amberlyst A21 is a promising adsorbent for dye removal from wastewater.
- Adsorption capacity of Amberlyst A21 for Remazol Brilliant Blue R was high compared to other adsorbent materials.
- Langmuir monolayer capacity of Amberlyst A21 was calculated as 208.33 mg/g.

✉ Hulya Silah
hulya.mercan@bilecik.edu.tr

[1] Department of Chemistry, Faculty of Art & Science, Bilecik Seyh Edebali University, 11210 Bilecik, Turkey

1 Introduction

Nowadays, different pollutants such as pesticides, dyes, heavy metals, and pharmaceuticals have contaminated the water resources due to agricultural applications, industrialization and rapid population growth (Vakili et al. 2019). Dyes are extensively used as a colorant in textile, plastic, leather, paper, rubber, printing, cosmetics, and food industries. Dyes are well-known water pollutants, which gives non-aesthetic or repelling look, and also various health problems for humans, animals and aquatic life (Suganya et al. 2017). Effluents with dye presence even at small concentrations (<1 mg/L) is highly discernible and recalcitrant (Jothirani et al. 2016). The large-scale production and widespread use of these dyes can cause serious environmental problems, making it an important public concern (Malik and Grohmann 2012). Thus, the effective removal of the dye Remazol Brilliant Blue R from water sources is highly desirable for environmental security and public health. Various physical, chemical and biological techniques, including adsorption (Senthamarai et al. 2013; Youcef et al. 2019; Gül and Silah 2014; Tharaneedhar et al. 2017), flocculation (Guo et al. 2019), ozonation (Hassani et al. 2019), advanced oxidation (Navarro et al. 2019), membrane filtration (Liu et al. 2018), ion-exchange (Wawrzkiewicz et al. 2018), photocatalytic degradation (Abdelrahman et al. 2019), and biosorption (Canizo et al. 2019) have been used for the treatment of dye containing water. Among these wastewater treatment methods, adsorption is attractive and considered to be promising because of its easy operation and lack of secondary pollution (Cui et al. 2019). Recently, the adsorption method has become more popular for wastewater treatment because of its efficiency in the removal of a wide range of pollutants that are stable to biological methods (Pavithra et al. 2019; Kyzas and Kostoglu 2014).

Anthraquinone dyes, which contain anthraquinone chromophore groups in the molecular structure, are mostly used within the textile industry. These dyes have complex and stable structures and are resistant to degradation (Li et al. 2019). The anthraquinone dye, Remazol Brilliant Blue R (RBBR), is one synthetic dye that is widely used in the textile industry and applied to fabric such as wool, nylon, and silk to ensure a wide range of colorfast and brilliant colors hues (Table 1). RBBR is further used in other dyeing processes such as paper and leather (Rahmat et al. 2016). The presence of dyes in water, especially azo and anthraquinones, causes serious risks for the environmental media and human health (Simoes et al. 2019).

Anion exchange Amberlyst A21 is a weak macroporous polystyrene resin, with an exchange capacity of 1.25 eq. L^{-1} and tertiary amines $-NR_2$ representing more than 85% of the functional groups (Dupoiron et al. 2018; Guimarães and Leão 2014). In the recent years,

Table 1 Properties of Remazol Brilliant Blue R

Molecular formula	Chemical structure	Molecular weight (g/mol)	CAS No.	λ_{max} (nm)
$C_{22}H_{16}N_2Na_2O_{11}S_3$	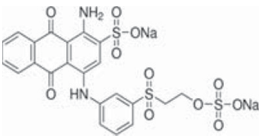	626.54	2580-78-1	590

there is an increasing interest in applying Amberlyst 21 as an adsorbent due to its specific physical and chemical structure as well as its highly selective properties. Amberlyst A21 resin has been used for the removal and recovery of various pollutants such as chromium (VI) (Karekar and Divekar 2017), palladium (II) (Hubicki and Wolowicz 2009; Nagireddi et al. 2018), zinc (Machado et al. 2015), sulphate (Guimarães and Leão 2014), $CoCl_2$ (Dunnewijk et al. 2006) acetic acid (Han et al. 2006; Sarı and Özmen 2018; Chen et al. 2017), phenol (Chen et al. 2017), butyric and oxalic acids (Sarı and Özmen 2018).

To the best of our knowledge, there are not many reports on using Amberlyst A21 adsorbent for removal of dyes. The main objectives of this manuscript were to evaluate the adsorption potential of a macroporous polystyrene resin called Amberlyst A21 surface for removal of RBBR from aqueous solutions and to investigate the adsorption isotherms and kinetics of RBBR. The morphology of Amberlyst A21 was analyzed by Fourier transform infrared spectroscopy (FTIR) and Scanning Electron Microscopy (SEM) techniques. The adsorption parameters for RBBR which affect dye removal, including solution pH, contact time, adsorbent dosage and initial concentration of RBBR, were investigated thoroughly. The adsorption mechanism of RBBR onto Amberlyst A21 adsorbent was determined by applying the Langmuir, Freundlich and Temkin isotherm models. Besides, the adsorption of RBBR was investigated kinetically to determine the adsorption rate in order to define the adsorption behavior.

2 Experimental

2.1 Materials

Amberlyst A21 (216410 CAS 9049-93-8) was supplied from Sigma-Aldrich (Germany) as an adsorbent. RBBR dye used as an adsorbate was also supplied by Sigma-Aldrich. Sodium hydroxide (NaOH) and hydrochloric acid (HCl) were purchased from Merck, Germany. All chemicals were used in analytical grade. Deionized water was used throughout the experiment.

2.2 Characterization of Amberlyst A21

The morphology of the Amberlyst A21 was investigated by using Scanning Electron Microscopy (SEM, Zeiss Supra 40 V). Before analysis, Amberlyst A21 was fixed on stubs by carbon tape and then coated with an Au/Pd layer. Additionally, Amberlyst A21 was characterized by FTIR. The FTIR of the Amberlyst A21 was conducted before and after adsorption of RBBR in the range 400–4000 cm^{-1} with resolution of 4 cm^{-1} using an FTIR spectrometer (Perkin Elmer, Spectrum 100 model). The samples were analyzed with ATR technique.

2.3 Batch Adsorption Characteristics of RBBR

A Remazol Brilliant Blue R stock solution of 1000 ppm was prepared by dissolving 1.0 g of RBBR dye in 1000 mL of deionized water. The desired pH value of solution was adjusted using hydrochloric acid (0.1 M) and sodium hydroxide (0.1 M). The adsorption experiments were conducted in batch to determine the optimal conditions for adsorption processes of RBBR on Amberlyst A21; solution pH (2.0–10.0), contact time (5–180 min), adsorbent dosage (0.25–2.00 g/L), and initial RBBR concentrations (50–250 ppm). For batch adsorption

experiments, a certain amount of Amberlyst A21 was added to 50 mL aqueous dye solutions of required initial RBBR concentration in Erlenmeyer flasks.

A T80 Model UV/VIS Spectrophotometer (PG Instruments) was used for determination of the concentration of RBBR in aqueous solutions. Value of λ_{max} for RBBR was taken as 590 nm. The amount of RBBR adsorbed on unit weight of Amberlyst A21 q_e (mg/g) was calculated by using the following equation:

$$q_e = \frac{(C_0 - C_e)}{m} V \tag{1}$$

where C_0 (ppm) and C_e (ppm) represent the initial and the equilibrium concentrations of RBBR dye, respectively, and V (L) is the volume of dye solution and m (g) is the mass of Amberlyst A21. Also, removal (%) of RBBR was calculated using the following equation:

$$Removal\ (\%) = \frac{(C_0 - C_e)}{C_0} 100 \tag{2}$$

For the measurement of the regeneration capacity of the Amberlyst A21, RBBR loaded materials were separated by centrifugation. RBBR loaded resin samples were washed in several cycles using deionized water. Thereafter, specific quantities of resins were kept in Erlenmayer flasks and a specific quantity of eluent volume (50 mL) was added and the mixture was subjected to mechanical shaking (100 rpm) at room temperature. Eventually, the final RBBR concentration was measured for the determination of desorption-based RBBR recovery.

2.4 Adsorption Isotherm and Kinetics Models

Isotherm and kinetics models of adsorption studies are of great importance to define the mode of adsorption process. In the present study, three isotherm models, i.e., Langmuir, Freundlich and Temkin, were used to investigate the equilibrium data of RBBR adsorption on the Amberlyst A21. Also, several kinetics models such as the pseudo-first order and pseudo-second order kinetic models were studied in detail.

3 Results and Discussion

3.1 Characterization of Amberlyst A21

The adsorption capacity of any adsorbent primarily depends on the adsorbent morphology such as the porosity and the functional groups available on adsorbent surface (Kumar et al. 2014a, b). Fourier transform infrared spectrophotometer (FTIR) was used to identify the different functional groups present on the Amberlyst A21. The FTIR of the Amberlyst A21 was taken before and after adsorption of RBBR. Figure 1 shows that the FTIR spectra of Amberlyst A21 and RBBR loaded Amberlyst A21.

As shown in Fig. 1, presence of C-H stretching vibrations of alkane was confirmed by its bending vibration peaks in the range of 3000–2850 cm^{-1} (at 2935 and 2857 cm^{-1}) for free Amberlyst A21 resin. Moreover, the band at 1362 cm^{-1} is an indication of the presence of C-N stretching vibration of amine. There are also bands characterizing aromatic stretching

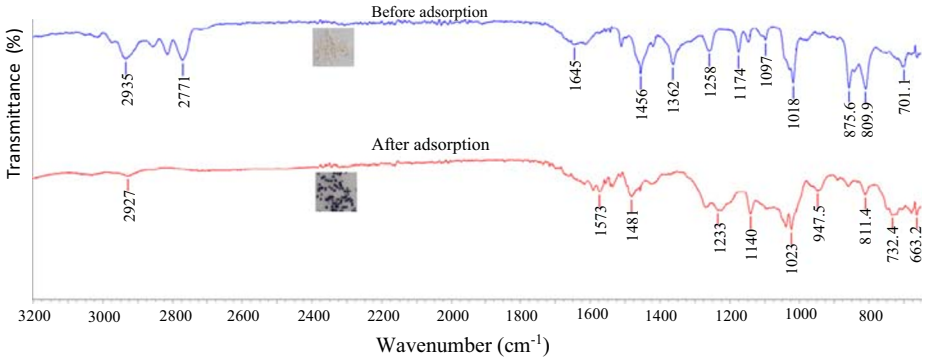

Fig. 1 FTIR spectra of free Amberlyst A21 and RBBR loaded Amberlyst A21

vibrations of C=C and = C-H bending vibrations of alkene assigned at 1600–1400 and 1000–675 cm^{-1}, respectively (Nagireddi et al. 2018). Meaningful shifts in the spectral peaks were observed when comparing the spectrum of Amberlyst A21 before and after RBBR adsorption. Noticeable new peaks were seen such as at 1573 cm^{-1}. These shifts occur due to the binding of RBBR ions with functional groups of Amberlyst A21 surface. Thus, changing of wavenumber of peaks confirms the adsorption of RBBR on the surface of Amberlyst A21.

SEM images of fresh and RBBR loaded Amberlyst A21 are presented in Fig. 2. Figure 2a shows the SEM image of pure Amberlyst A21, where some porous structure is seen on the surface of Amberlyst A21. In Fig. 2b, the RBBR adsorbed by the adsorbent surface can be clearly visible. After the dye adsorption, surface of Amberlyst A21 appears smoother. The results observed from the SEM analysis identified that Amberlyst A21 has an appropriate morphology for RBBR dye adsorption.

3.2 Effect of Solution pH and Contact Time

The adsorption of organic species and metals is significantly affected by the solution pH, because pH determines properties of adsorbent and adsorbate molecules such as the surface charge of the adsorbent and ionization degree of the adsorbate molecule. Therefore, the effect of solution pH on RBBR adsorption onto Amberlyst A21 was studied in the pH range from 2.0 to 10.0. Figure 3a indicates that the adsorption efficiency of RBBR dye by Amberlyst A21

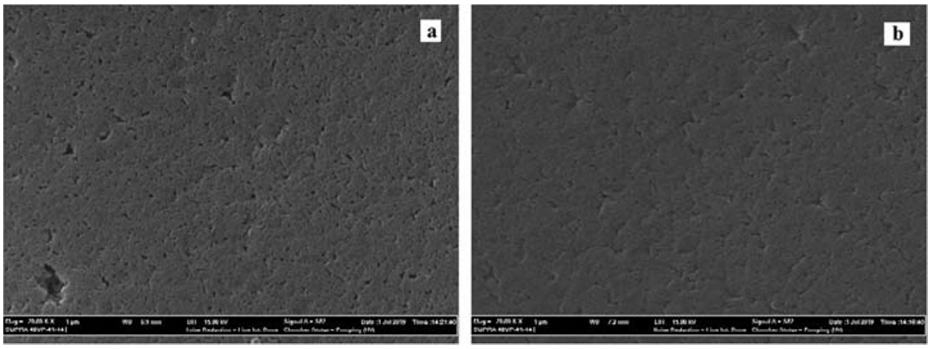

Fig. 2 SEM images of (**a**) fresh Amberlyst A21, and **b** RBBR loaded Amberlyst A21 resin

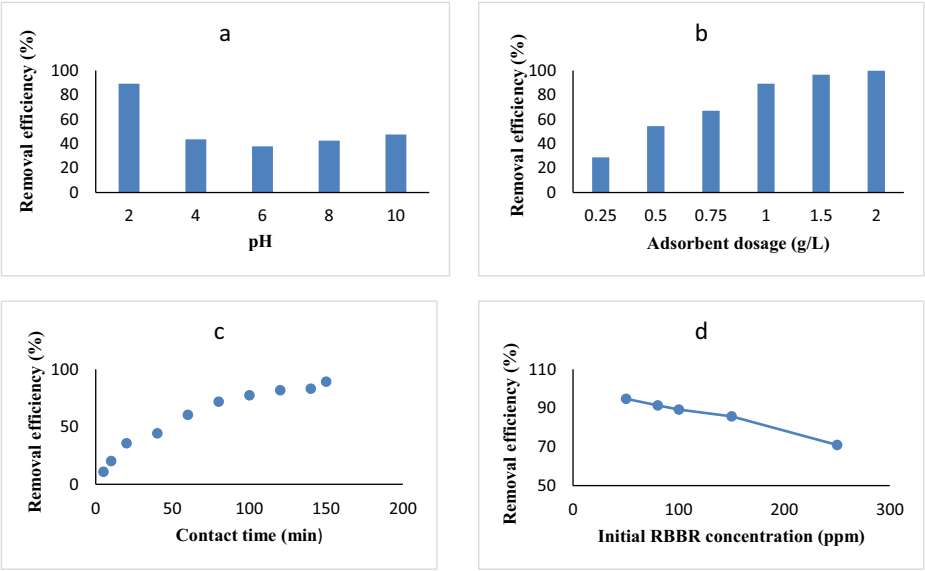

Fig. 3 Effect of (**a**) solution pH, **b** adsorbent dosage, **c** contact time, and **d** initial dye concentration on the removal percent of RBBR dye using by Amberlyst A21 adsorbent

decreased as solution pH increased, and at pH 2 Amberlyst A21 adsorbent had the highest removal rate at 89.23% for 100 ppm initial RBBR concentration.

It can be seen that the removal of RBBR on to the surface of Amberlyst A21 adsorbent is dependent on solution pH, which is similar to previous results in the literature (Jiang et al. 2014; Saputra et al. 2017). In the presence of H^+, the primary amino groups existing on the Amberlyst A21 adsorbent become protonated, as seen as Fig. 4 (Nagireddi et al. 2018; Saputra et al. 2017). Simultaneously, the RBBR is dissolved in an aqueous solution after which its contained sulfonate groups (Dye-SO_3Na) become dissociated and converted into anionic dye

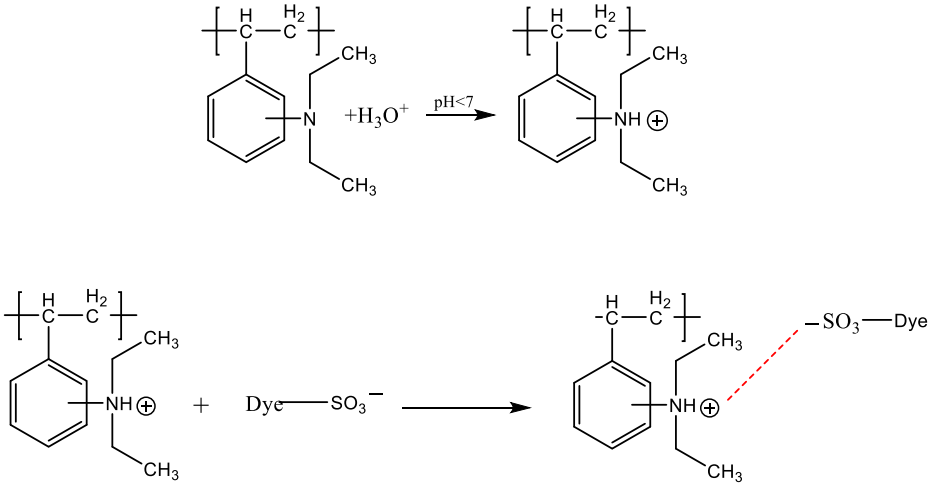

Fig. 4 Adsorption mechanism of RBBR on to the Amberlyst A21 surface

ions (Dye-SO_3^-). In this situation, strong electrostatic interaction exists between the cationic Amberlyst A21 adsorbent and anionic RBBR dye ions (Jiang et al. 2014). When the pH of the solution changed from 2 to 6, the adsorption efficiency significantly decreased from 89.23% to 37.75%. The reduction in the adsorption of dye at pH greater than 2 can be attributed to the decrease of the positively charged sites on the surface of the Amberlyst A21 at alkaline medium. Moreover, the competitions for adsorption on active sites of Amberlyst A21 occurred between anionic RBBR dye ions and hydroxyl ions with increasing pH of solution. It is seen that this experimental data is consistent with the literature (Guimarães and Leão 2014). Electrostatic attraction between the charged surface and charged dye molecule may be considered as the principal adsorption mechanism.

The other important factor of adsorption experiments that strongly effects the removal of dyes is the contact time (Fig. 3c). Effects of contact time on RBBR adsorption by Amberlyst A21 was evaluated from 5 to 180 min at 100 ppm initial dye concentration with a fixed Amberlyst A21 dosage (1.0 g/L) at pH 2.0. When the contact time increased from 5 to 60 min, the adsorption percent of RBBR increased from 11.10 to 60.39%, and the adsorption reached equilibrium at about 150 min with 89.23% of removal efficiency. The experimental results showed that the adsorption percent values of RBBR did not change much in contact times after 150 min. This observation may be explained by the presence of more than enough adsorption binding sites on the surface of Amberlyst A21 that simplifies rapid attachment of RBBR ions on Amberlyst A21 surface and penetration in the Amberlyst A21 pores in short time (Yusuff 2019). Thus, an optimal contact time of 150 min was selected for further adsorption studies of RBBR.

3.3 Effect of Adsorbent Dosage

Adsorbent amount is one of the main experimental parameters to determine the capacity uptake of dyes by adsorbents. The effect of adsorbent amount on the uptake of RBBR dye was studied in the range from 0.25 to 2.00 g/L while keeping the other experimental conditions constant. It was seen that the removal percent of 100 ppm RBBR ions increased from 28.76 to 99.80% with the increase in Amberlyst dosage from 0.25 to 2.00 g/L. The result is similar with previous studies and this can be attributed to the increase of the number of active binding sites and surface area of the adsorbent with the increase of the amount of the adsorbent (Kumar et al. 2014a, b; Sathishkumar et al. 2012). As shown in Fig. 3b, further increase in Amberlyst A21 dosage after 1.50 g/L did not cause significant improvement in removal efficiency. This may be due to the binding of RBBR ions to the adsorbent and the establishment of equilibrium between the RBBR ions bound to the sorbent and those remaining unadsorbed by Amberlyst A21 in the aqueous solution. For adsorption of RBBR on Amberlyst A21, the adsorbent dosage was chosen as 1.0 g/L with the percent removal of 89.23% at 100 ppm initial dye concentration.

3.4 Effect of the Initial RBBR Concentration

The initial concentrations of dyes in the solution significantly effects dye adsorption. The affect of the initial RBBR concentration on the removal performance of Amberlyst A21 was studied in the concentration range from 50 to 250 ppm using a 1.00 g/L Amberlyst A21 dosage at 25 °C. The percent adsorption decreased from 94.84% to 70.98% as the initial RBBR concentration increased from 50 to 250 ppm (Fig. 3d). This may be due to saturation of the

adsorption sites and increase in the number of RBBR ions competing for the available binding sites on the Amberlyst A21 surface. Also, the equilibrium adsorption capacity for Amberlyst A21 was increased from 47.54 to 177.45 mg/g as the RBBR concentration in the solution was increased from 50 to 250 ppm. This phenomenon is due to an increase in the driving force of the concentration gradient, as an increase in the initial dye concentration (Kumar and Ramalingam 2013).

3.5 Adsorption Isotherm Study

Adsorption isotherm models are a description of the relationship between the adsorbate-adsorbent interactions at given temperature under equilibrium conditions; these models help the design of adsorption procedures (Ahmed et al. 2019; Kallel et al. 2016). To understand the adsorption mechanism of RBBR from an aqueous solution by the Amberlyst A21, we studied several adsorption isotherm models, and three, i.e., Langmuir, Freundlich and Temkin, were used to define the most appropriate isotherm model for the adsorption of RBBR onto Amberlyst A21. The Langmuir isotherm model is one of the most extensively applied models in adsorption studies to describe the adsorption of an adsorbate onto solid adsorbent surface. This isotherm model assumes that adsorption is limited to one monolayer, the energy of sorption is equal for all binding sites, and the adsorption of adsorbate ions is a process occurring on a homogenous adsorbent surface without any interplay between adsorbed ions (Can et al. 2016). Also, the maximum adsorption capacity (q_{max}) of adsorbents can be investigated using by the Langmuir adsorption isotherms. The Langmuir isotherm equation can be expressed as follows (Langmuir 1918):

$$\frac{C_e}{q_e} = \frac{C_e}{q_{max}} + \frac{1}{q_{max} K_L} \tag{3}$$

Freundlich isotherm model is applied to heterogeneous adsorbent surface where the active binding sites are nonequivalent and multiple adsorptive layers occur on interaction between adsorbate molecules (Siddiqui et al. 2019). The equation of Freundlich isotherm model is as follows (Freundlich 1906):

$$lnq_e = lnK_F + \frac{1}{n_F} lnC_e \tag{4}$$

The Temkin isotherm model was widely used to decide the free energy of adsorption as a function of adsorbent surface coverage assuming a uniform distribution of the binding energy and the heat of the adsorption of all adsorbate molecules in the layer decreases linearly rather than logarithmically with the surface of adsorbent coverage due to adsorbate-adsorbent interactions (Jasni et al. 2017). The Temkin isotherm model is given as follows:

$$q_e = A\ lnK_T + A\ lnC_e \tag{5}$$

In the above equations, q_{max} is the maximum adsorption capacity (mg/g), q_e is the adsorption capacity (mg/g), K_L is the Langmuir constant (L/mg), K_F is the Freundlich constant and n_F is a parameter related to adsorbate-adsorbent affinity, K_T is the Temkin isotherm equilibrium binding constant, A is the constant related to heat of adsorption.

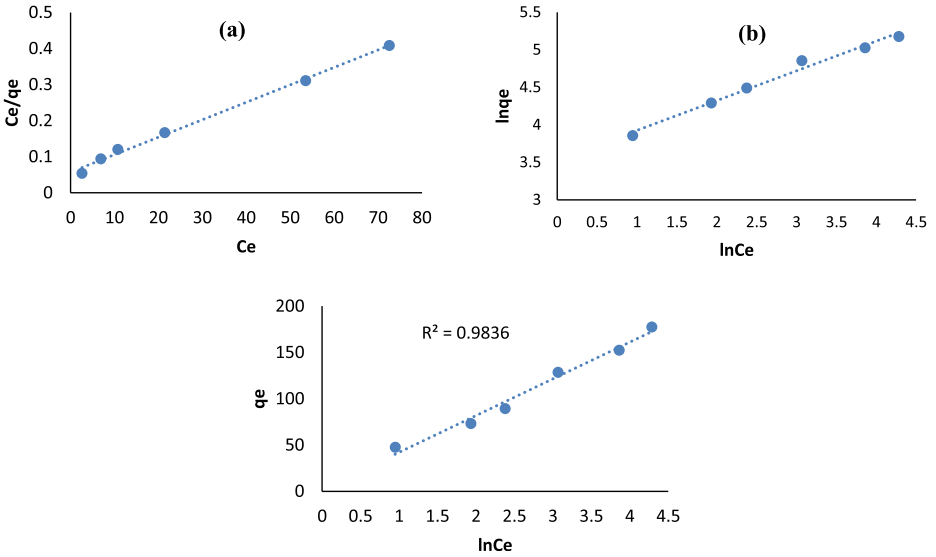

Fig. 5 Isotherm models of (**a**) Langmuir, **b** Freundlich, and **c** Temkin for the adsorption of RBBR on Amberlyst A21

Equilibrium isotherm graphs and parameters for RBBR dye were obtained at pH 2.0 and 25 °C (Fig. 5). The Langmuir, Freundlich and Temkin adsorption parameters calculated for RBBR are presented in Table 2.

The data showed that the RBBR adsorption process was well defined by the Langmuir adsorption isotherm model, and better than the Freundlich and Temkin adsorption isotherm models, based on the higher determination coefficient (R^2) values obtained for the Langmuir model (0.9954 compared to 0.9852 and 0.9836, respectively). So, the adsorption isotherm of RBBR onto Amberlyst A21 fits better the Langmuir isotherm model. The result shows that adsorption of RBBR on Amberlyst A21 occurs on a homogenous surface by monolayer coverage (Janaki et al. 2012). Also, the Langmuir isotherm model was used to estimate the maximum adsorption capacity (q_{max}) corresponding to complete monolayer coverage on the Amberlyst A21 surface. q_{max} determined from the Langmuir isotherm defines the total capacity of the Amberlyst A21 for the RBBR as 208.33 mg/g. This value was also comparable to the adsorption capacities of some other adsorbent materials for RBBR (Table 3). Amberlyst A21 showed a higher adsorption capacity compared to the amino functionalized organosilane, mesoporous active carbon, and magnetite nanoparticles. The easier preparation conditions and relatively high adsorption capacity suggest that Amberlyst A21 is a potential adsorbent material for dye removal from aqueous solutions.

Table 2 Isotherm parameters of Langmuir, Freundlich and Temkin models for RBBR adsorption on Amberlyst A21

Langmuir	Equation	R^2	q_{max}	K_L	
	$\frac{C_e}{q_e} = 0.0048\ C_e + 0.0576$	0.9954	208.33	0.083	
Freundlich	Equation	R^2	1/n	n_F	K_F
	$\ln q_e = 0.3968\ \ln C_e + 3.5284$	0.9852	0.3968	2.52	34.07
Temkin	Equation	R^2	A	K_T	
	$q_e = 39.668\ \ln C_e + 2.5286$	0.9836	23.14	1.61	

Table 3 Comparison of maximum dye adsorption capacities for RBBR by several adsorbents

Adsorbent	q_{max} (mg/g)	References
Amino functionalized organosilane	21.30	Saputra et al. (2017)
Mesoporous activated carbon	33.47	Silva et al. (2016)
Magnetite nanoparticles	74.40	Khoshhesab and Modaresnia (2019)
Biochar derived from Turbinaria conoides	85.30	Vijayaraghavan and Ashokkumar (2019)
Amberlyst A21	208.33	This study
Poly[2-hydroxy-3-(1-naphthyloxy)propyl]methacrylate	238.10	Torgut et al. (2017)
ZnO powder	345.00	Ada et al. (2009)

According to the Freundlich isotherm model, the significance of the n_F value is as follows: $n_F < 1$ means that adsorption is a chemical process, $n_F = 1$ means that adsorption is linear, and $n_F > 1$ means that adsorption is a physical process (Kumar et al. 2014a, b). The obtained n_F value for the RBBR-Amberlyst A21 system was 2.52. This confirms that the adsorption of RBBR dye on Amberlyst A21 is a physical process.

An important characteristic of the Langmuir isotherm model concerns the separation factor (R_L) which is a dimensionless parameter specifying the adsorption phenomenon. It can be calculated from the following equation:

$$R_L = \frac{1}{1 + K_L\, C_0} \tag{6}$$

where K_L is a Langmuir isotherm constant and C_0 is the initial RBBR concentration. The value of R_L provides an indication on if the adsorption phenomenon is favorable ($0 < R_L < 1$), unfavorable ($R_L > 1$), linear ($R_L = 1$) or irreversible ($R_L = 0$). In this regard, the dimensionless parameters were calculated for the adsorption of RBBR on Amberlyst A21 in the range 0.057–0.194 for dye, suggesting that the adsorption process is favorable (Satılmış and Uyar 2018) and Amberlyst A21 can be used for RBBR removal.

The Temkin isotherm model defines the interactions between adsorbent and adsorbate assuming that the free energy sorption is a function of the surface coverage. The obtained values (Table 2) for Temkin isotherm model confirm the strong interaction between the reactive functional groups on the Amberlyst A21 surface and RBBR ions.

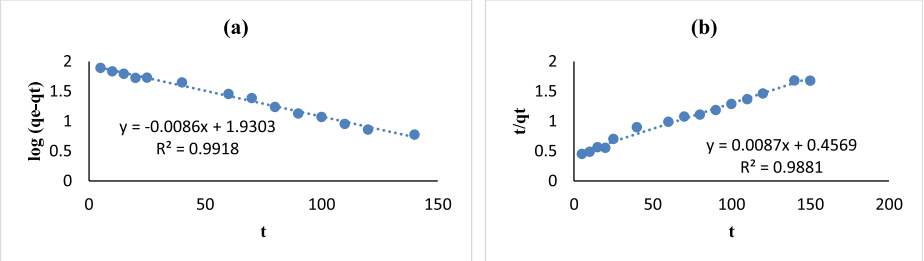

Fig. 6 Kinetic models of (**a**) pseudo first-order and **b** pseudo second-order for the adsorption of RBBR

Table 4 Kinetic parameters for the adsorption of RBBR onto Amberlyst A21

			Pseudo first-order kinetic model			Pseudo second-order kinetic model		
	Initial concentration (ppm)	qe_{exp} (mg/g)	qe_{cal} (mg/g)	k_1 (min^{-1})	R^2	qe_{cal} (mg/g)	k_2 (g/mg dak)	R^2
Amberlyst A21	80	69.04	63.59	2.23×10^{-4}	0.9810	86.21	2.96×10^{-4}	0.9871
	100	87.45	85.17	1.98×10^{-4}	0.9918	114.94	1.66×10^{-4}	0.9881
	150	128.54	138.04	2.49×10^{-4}	0.9645	164.20	1.40×10^{-4}	0.9825

3.6 Adsorption Kinetics

To determine the maximum adsorption capacity of adsorbents, two types of kinetics models are widely used and compared, namely the pseudo first-order and pseudo second-order kinetic model. The equations of these kinetics models are respectively given as follows (Ho and Mckay 1999):

$$\log(q_e - q_t) = -\frac{k_1}{2.303}t + \log q_e \tag{7}$$

$$\frac{t}{q_t} = \frac{1}{k_2 q_e^2} + \frac{1}{q_e}t \tag{8}$$

where q_e and q_t are the amount of RBBR adsorbed onto Amberlyst A21 at equilibrium and any t time (mg/g), and k_1 and k_2 are the rate constants of pseudo first-order and pseudo second-order, respectively.

Kinetic graphs and data for adsorption of RBBR on Amberlyst A21 were obtained at pH 2.0 and 25 °C (Fig. 6). Parameters of the pseudo first- and pseudo second-order kinetic model calculated for RBBR are given in Table 4.

As shown in Table 4, experimental data of kinetic studies showed that the theoretical q_e value (qe_{cal}) from pseudo first-order kinetic model was more consistent with the experimental q_e value (qe_{exp}) than that calculated from the pseudo second-order kinetic model. Also, the value of the determination coefficient R^2 acquired from the pseudo first-order kinetic model was 0.9918 and higher than that from the other kinetic model. For these reasons, the kinetics of adsorption of RBBR onto Amberlyst A21 is described better with the pseudo first-order kinetic model well. The pseudo first-order model is the earliest developed equation that explains reversible equilibrium between adsorbate and adsorbent. It also assumes that the rate in which the sites become occupied is exactly equal to number of vacant sites (Awad et al. 2019).

3.7 Desorption Studies

Adsorption of RBBR was conducted at the optimal pH condition (pH = 2) and desorption was conducted at 0.1 M NaOH and 0.1 M KOH. The RBBR desorption efficiency was found to be 61.3% and 60.0%, respectively. The significant amount of RBBR desorbed from the RBBR-loaded Amberlyst A21 at 0.1 M NaOH and 0.1 M KOH can be helpful for recycling the spent adsorbent.

4 Conclusions

In this study, a macroporous polystyrene resin, Amberlyst A21, was used as an adsorbent for the removal of Remazol Brilliant Blue R. Under optimal adsorption conditions, i.e., solution pH 2.0, 150 min contact time at 25 °C, and adsorbent dosage 1.0 g/L, the maximum adsorption capacity was determined at 208.33 mg/g. The adsorption isotherm studies showed that the adsorption of Remazol Brilliant Blue R is described well by the Langmuir isotherm model. Also, calculated values of the R_L showed that the adsorption of Remazol Brilliant Blue R onto Amberlyst A21 was favorable. The kinetic analyses indicate that the adsorption of dye follows a pseudo first-order kinetic model. Amberlyst A21 as a potential and good adsorbent is promising for removal of dyes from wastewater.

Acknowledgements G. Ozturk would like to thank the Science Fellowships and Grant Programmes Department (BIDEB) of The Scientific and Technological Research Council of Turkey (TUBITAK) for the graduate scholarship of 2210-C National Priority Areas MSc Scholarship Program.

Compliance with Ethical Standards

The authors declare that they have no conflict of interest.

References

Abdelrahman EA, Hegazey RM, Kotp YH, Alharbi A (2019) Facile synthesis of Fe_2O_3 nanoparticles from Egyptian insecticide cans for efficient photocatalytic degradation of methylene blue and crystal violet dyes. Spectrochim Acta A 222(117195):1–11. https://doi.org/10.1016/j.saa.2019.117195

Ada K, Ergene A, Tan S, Yalçın E (2009) Adsorption of Remazol Brilliant Blue R using ZnO fine powder: equilibrium, kinetic and thermodynamic modeling studies. J Hazard Mater 165(1–3):637–644. https://doi.org/10.1016/j.hazmat.2008.10.036

Ahmed AM, Ali AE, Ghazy AH (2019) Adsorption separation of nickel from wastewater by using olive stones. Adv J Chem A 2:79–93. https://doi.org/10.29088/SAMI/AJCA.2019.2.7993

Awad AM, Shaikh SMR, Jalab R, Gulied MH, Nasser MS, Benamor A, Adham S (2019) Adsorption of organic pollutants by natural and modified clays: a comprehensive review. Sep Purif Technol 228:115719. https://doi.org/10.1016/j.seppur.2019.115719

Can N, Ömür BC, Altındal A (2016) Modeling of heavy metal ion adsorption isotherms onto metallophthalocyanine film. Sensor Actuat B-Chem 237:953–961. https://doi.org/10.1016/j.snb.2016.07.026

Canizo BV, Agostini E, Wevar Oller AL, Dotto GL, Vega IA, Escudero LB (2019) Removal of crystal violet from natural water and effluents through biosorption on bacterial biomass isolated from rhizospheric soil. Water Air Soil Poll 230(210):1–14. https://doi.org/10.1007/s11270-019-4235-5

Chen K, Hao S, Lyu H, Luo G, Zhang S, Chen J (2017) Ion exchange separation for recovery of monosaccharides, organic acids and phenolic compounds from hydrolysates of lignocellulosic biomass. Sep Purif Technol 172:100–106. https://doi.org/10.1016/j.seppur.2016.08.004

Cui W, Kang X, Zhang X, Cui X (2019) Gel-like ZnO/Zr-MOF(bpy) nanocomposite for highly efficient adsorption of Rhodamine B dye from aqueous solution. J Phys Chem Solids 134:165–175. https://doi.org/10.1016/j.jpcs.2019.06.004

Dunnewijk J, Bosch H, de Haan AB (2006) Adsorption kinetics of $CoCl_2$ and PPh_3 over macroreticular and gel type adsorbents by a generalized ZLC method. Chem Eng Sci 61:4813–4826. https://doi.org/10.1016/j.ces.2006.03.013

Dupoiron S, Lameloise M, Bedu M, Lewandowski R, Fargues C, Allais F, Teixeira ARS, Rakotoarivonina H, Remond C (2018) Recovering ferulic acid from wheat bran enzymatic hydrolysate by a novel and non-thermal process associating weak anion-exchange and electrodialysis. Sep Purif Technol 200:75–83. https://doi.org/10.1016/j.seppur.2018.02.031

Freundlich HMF (1906) Over the adsorption in solution. J Phys Chem 57:385–471
Guimarães D, Leão VA (2014) Batch and fixed-bed assessment of sulphate removal by the weak base ion exchange resin Amberlyst A21. J Hazard Mater 280:209–215. https://doi.org/10.1016/j.jhazmat.2014.07.071
Gül UD, Silah H (2014) Comparison of color removal from reactive dye contaminated water by systems containing fungal biosorbent, active carbon and their mixture. Water Sci Technol 70:1168–1174. https://doi.org/10.2166/wst.2014.339
Guo K, Gao B, Tian X, Yue Q, Zhang P, Shen X, Xu X (2019) Synthesis of polyaluminium chloride/papermaking sludge-based organic polymer composites for removal of disperse yellow and reactive blue by flocculation. Chemosphere 231:337–348. https://doi.org/10.1016/j.chemosphere.2019.05.138
Han B, Carvalho W, Canilha L, da Silva SS, e Silva JBA, McMillan JD, Wickramasinghe SR (2006) Adsorptive membranes vs. resins for acetic acid removal from biomass hydrolysates. Desalination 193:361–366. https://doi.org/10.1016/j.desal.2007.09.080
Hassani KE, Kalnina D, Turks M, Beakou BH, Anouar A (2019) Enhanced degradation of an azo dye by catalytic ozonation over Ni-containing layered double hydroxide nanocatalyst. Sep Purif Technol 210:764–774. https://doi.org/10.1016/j.seppur.2018.08.074
Ho YS, Mckay G (1999) Pseudo-second order model for sorption processes. Process Biochem 34:451–465. https://doi.org/10.1016/S0032-9592(98)00112-5
Hubicki Z, Wolowicz A (2009) Adsorption of palladium (II) from chloride solutions on Amberlyst A29 and Amberlyst A21 resins. Hydrometallurgy 96:159–165. https://doi.org/10.1016/j.hydromet.2008.10.002
Janaki V, Vijayaraghavan K, Ramasamy AK, Lee KJ, Oh BT, Kamala-Kannan S (2012) Competitive adsorption of reactive Orange 16 and reactive brilliant blue R on polyaniline/bacterial extracellular polysaccharides composite-a novel eco-friendly polymer. J Hazard Mater 241-242:110–117. https://doi.org/10.1016/j.jhazmat.2012.09.019
Jasni MJF, Arulkumar M, Sathishkumar P, Yusoff ARM, Buang NA, Gu FL (2017) Electrospun nylon 6,6 membrane as a reusable nano-adsorbent for bisphenol a removal: adsorption performance and mechanism. J Colloid Interf Sci 508:591–602. https://doi.org/10.1016/j.jcis.2017.08.075
Jiang X, Sun Y, Liu L, Wang S, Tian X (2014) Adsorption of C.I. reactive blue 19 from aqueous solutions by porous particles of the grafted chitosan. Chem Eng J 235:151–157. https://doi.org/10.1016/j.cej/2013.09.001
Jothirani R, Senthil Kumar P, Saravanan A, Narayan AS, Dutta A (2016) Ultrasonic modified corn pith for the sequestration of dye from aqueous solution. J Ind Eng Chem 39:162–175. https://doi.org/10.1016/j.jiec.2016.05.024
Kallel F, Chaari F, Bouaziz F, Bettaieb F, Ghorbel R, Chaabouni SE (2016) Sorption and desorption characteristics for the removal of a toxic dye, methylene blue from aqueous solution by a low cost agricultural by-product. J Mol Liq 219:279–288. https://doi.org/10.1016/j.molliq.2016.03.024
Karekar JM, Divekar SV (2017) Adsorption studies of chromium (VI) on weak base resins Tulsion A-10X (MP) and Amberlyst A-21 (MP) in aqueous and mixed media. Desalin Water Treat 82:252–261. https://doi.org/10.5004/dwt.2017.20992
Khoshhesab ZM, Modaresnia N (2019) Adsorption of acid black and Remazol Brilliant Blue R onto magnetite nanoparticles. Inorg Nano-Met Chem 49(8):231–239. https://doi.org/10.1080/24701556.2019.1659820
Kumar PS, Ramalingam S (2013) Process optimization studies of Congo red dye adsorption onto cashew nut shell using response surface methodology. Int J Ind Chem 4:17–10. https://doi.org/10.1186/2228-5547-4-17
Kumar SP, Fernando PSA, Ahmed RT, Srinath R, Priyadharshini M, Vignesh AM, Thanjıappan A (2014a) Effect of temperature on the adsorption of methylene blue dye onto sulfuric acid treated orange peel. Chem Eng Comm 201:1526–1547. https://doi.org/10.1080/00986445.2013.819352
Kumar PS, Senthamarai C, Durgadevi A (2014b) Adsorption kinetics, isotherm, and thermodynamic analysis of copper ions onto the surface modified agricultural waste. Environ Prog Sustain 33:28–37. https://doi.org/10.1002/ep.11741
Kyzas GZ, Kostoglu M (2014) Green adsorbents for wastewaters: a critical review. Materials 7:333–364. https://doi.org/10.3390/ma7010333
Langmuir I (1918) Adsorption of gases on plane surfaces of glass mica and platinum. J Am Chem Soc 40:1361–1403. https://doi.org/10.1021/ja02242a004
Li H, Wang Y, Wang Y, Wang H, Sun K, Lu Z (2019) Bacterial degradation of anthraquinone dyes. J Zhejiang Univ-Sc B 20:528–540. https://doi.org/10.1631/jzus.B1900165
Liu Y, Zhu W, Guan K, Peng C, Wu J (2018) Freeze-casting of alumina ultra-filtration membranes with good performance for anionic dye separation. Ceram Int 44:11901–11904. https://doi.org/10.1016/j.ceramint.2018.03.160
Machado RM, Gameiro MLF, Krupa M, Rodrigues JMA, Ismael MRC, Reis MTA, Carvalho JMR (2015) Selective separation and recovery of zinc and lead from galvanizing industrial effluents by anion exchange. Sep Sci Technol 50:2726–2736. https://doi.org/10.1080/01496395.2015.1062029
Malik A, Grohmann E (2012) Environmental protection strategies for sustainable development. Springer, New York

Nagireddi S, Golder AK, Uppaluri R (2018) Role of protonation and functional groups in Pd(II) recovery and reuse characteristics of commercial anion exchange resin-synthetic electroless plating solution systems. J Water Process Eng 22:227–238. https://doi.org/10.1016/j.jwpe.2018.02.008

Navarro P, Pellicer JA, Gomez-Lopez VM (2019) Degradation of azo dye by an UV/H_2O_2 advanced oxidation process using an amalgam lamp. Water Environ J 33:476–483. https://doi.org/10.1111/wej.12418

Pavithra KG, Senthil Kumar P, Jaikumar V, Rajan PS (2019) Removal of colorants from wastewater: a review on sources and treatment strategies. J Ind Eng Chem 75:1–19. https://doi.org/10.1016/j.jiec.2019.02.011

Rahmat NA, Ali AA, Salmiati Hussain N, Muhamad MS, Kristanti RA, Hadibarata T (2016) Removal of Remazol Brilliant Blue R from aqueous solution by adsorption using pineapple leaf powder and lime peel powder. Water Air Soil Poll 227(105):1–11. https://doi.org/10.1007/s11270-016-2807-1

Saputra OA, Rachma AH, Handayani DS (2017) Adsorption of Remazol Brilliant Blue R using amino-functionalized organosilane in aqueous solution. Indones J Chem 17(3):343-350. https://doi.org/10.22146/ijc.25097

Sarı SK, Özmen D (2018) Design of optimum response surface experiments for the adsorption of acetic, butryic, and oxalic acids on Amberlyst A21. J Disper Sci Technol 39:305–309. https://doi.org/10.1080/01932691.2017.1316208

Sathishkumar P, Arulkumar M, Palvannan T (2012) Utilization of agro-industrial waste *Jatropha curcas* pods as an activated carbon for the adsorption of reactive dye Remazol Brilliant Blue R (RBBR). J Clean Prod 22:67–75. https://doi.org/10.1016/j.jclepro.2011.09.017

Satılmış B, Uyar T (2018) Amine modified electrospun PIM-1 ultrafine fibers for an efficient removal of methyl orange from an aqueous system. Appl Surf Sci 453:220–229. https://doi.org/10.1016/j.apsusc.2018.05.069

Senthamarai C, Kumar PS, Priyadharshini M, Vijayalakshmi P, Kumar VV, Baskaralingam P, Thiruvengadaravi KV, Sivanesan S (2013) Adsorption behavior of methylene blue dye onto surface modified *Strychnos potatorum* seeds. Environ Prog Sustain 32(3):624–632. https://doi.org/10.1002/ep.11673

Siddiqui SI, Manzoor O, Mohsin M, Chaudhry SA (2019) *Nigella sativa* seed based nanocomposite-MnO_2/BC: an antibacterial material for photocatalytic degradation, and adsorptive removal of methylene blue from water. Environ Res 171:328–340. https://doi.org/10.1016/j.envres.2018.11.044

Silva TL, Ronix A, Pezoti O, Souza LS, Leandro PKT, Bedin KC, Beltrame KK, Cazetta AL, Almeida VC (2016) Mesoporous activated carbon from industrial laundry sewage sludge: adsorption studies of reactive dye Remazol Brilliant Blue R. Chem Eng J 303:467–476. https://doi.org/10.1016/j.cej.2016.06.009

Simoes MF, Maiorano AE, dos Santos JG, Peixoto L, de Souza RFB, Neto AO, Brito AG, Ottoni CA (2019) Microbial fuel cell-induced production of fungal laccase to degrade the anthraquinone dye Remazol Brilliant Blue R. Environ Chem Lett 17:1413–1420. https://doi.org/10.1007/s10311-019-00876-y

Suganya S, Senthil Kumar P, Saravanan A, Sundar Rajan P, Ravikumar C (2017) Computation of adsorption parameters for the removal of dye from wastewater by microwave assisted sawdust: theoretical and experimental analysis. Environ Toxicol Phar 50:45–57. https://doi.org/10.1016/j.etap.2017.01.014

Tharaneedhar V, Senthil Kumar P, Saravanan A, Ravikumar C, Jaikumar V (2017) Prediction and interpretation of adsorption parameters for the sequestration of methylene blue dye from aqueous solution using microwave assisted corncob activated carbon. SM&T 11:1–11. https://doi.org/10.1016/j.susmat.2016.11.001

Torgut G, Tanyol M, Biryan F, Pihtili G, Demirelli K (2017) Application of response surface methodology for optimization of Remazol Brilliant Blue R removal onto a novel polymeric adsorbent. J Taiwan Inst Chem E 80:406–414. https://doi.org/10.1016/j.jtice.2017.07.030

Vakili M, Deng S, Cagnetta G, Wang W, Meng P, Liu D, Yu G (2019) Regeneration of chitosan-based adsorbents used in heavy metal adsorption: a review. Sep Purif Technol 224:373–387. https://doi.org/10.1016/j.seppur.2019.05.040

Vijayaraghavan K, Ashokkumar T (2019) Characterization and evaluation of reactive dye adsorption onto biochar derived from Turbinaria conodies biomass. Environ Prog Sustain 38(4):1–9. https://doi.org/10.1002/ep.13143

Wawrzkiewicz M, Hubicki Z, Polska-Adach E (2018) Strongly basic anion exchanger Lewatit MonoPlus SR-7 for acid, reactive, and direct dyes removal wastewaters. Sep Sci Technol 53:1065–1075. https://doi.org/10.1080/01496395.2017.1293098

Youcef LD, Belaroui LS, Lopez-Galindo A (2019) Adsorption of a cationic methylene blue dye on an Algerian palygorskite. Appl Clay Sci 179(105145):1–10. https://doi.org/10.1016/j.clay.2019.105145

Yusuff AS (2019) Adsorption of hexavalent chromium from aqueous solution by Leucaena leucocephala seed pod activated carbon: equilibrium, kinetic and thermodynamic studies. Arab J Basic Appl Sci 26:89–102. https://doi.org/10.1080/25765299.2019.1567656